ISSN 2395-1621

Enhancement of heat transfer rate and thermal efficiency of solar air heater by using flow turbulator on absorber plate

[#1] M.M. Nagargoje, [#2]S.K. Bhor

[1]maheshnagargoje8087@gmail.com
[2]bhorguruji@yahoo.com

[#1]PG Student, Department of Mechanical Engineering, Dr. D Y Patil School of Engineering Academy, ambi,savitribai phule pune university, MH, India.
[#2]Assistant Professor, Department of Mechanical Engineering, Dr. D Y Patil Institute of Engineering and Technology,Pune savitribai phule pune university, MH, India.

ABSTRACT

Heat energy plays most important role in the field of power generation which involves the heat transfer in domestic as well as industrial purposes. The heat transfer coefficient between heat transferring surface and air is low which leads to lower thermal efficiency of the system. Therefore it is important to increase heat transfer coefficient between heat transferring surface and air. Artificial roughness applied on the absorber plate is the most acclaimed method to improve thermal performance of solar air heaters at the cost of low to moderate friction penalty. Experimental investigations pertinent to distinct roughness geometries unfolds that the enhancement in heat transfer is accompanied by considerable rise in pumping power. This work covers the types of technique used in enhance heat transfer coefficient in field of heat transfer and review a variety of papers dealing with artificial roughness on heat transfer field. The simplest and the most efficient way to utilize solar energy is to convert it into thermal energy for heating applications by using solar collectors. Solar collectors are special kind of heat exchangers that transform solar radiation energy to internal energy of the transport medium. The major component of any solar system is the solar collector. This is a device which absorbs the incoming solar radiation, converts it into heat and transfers this heat to a fluid (usually air, water, or oil) flowing through the collector. The solar energy thus collected is carried from the circulating fluid either directly to the hot water or space conditioning equipment or to a thermal energy storage tank from which can be drawn for use at night and/or cloud days. Solar air heaters, because of their inherent simplicity are cheap and most widely used collector devices.

***Keywords*— roughness, Solar air heater, Roughness geometry, thermal performance.**

ARTICLE INFO

Article History

Received :18th November 2015

Received in revised form :

19th November 2015

Accepted : 21st November , 2015

Published online :

22nd November 2015

I. INTRODUCTION

Energy is a basic need for human being. it is a prime agent in the generation and economic development. Energy resources may be classified in two ways conventional and non-conventional energy resources. Solar energy is available abundance on earth in the form of radiation. Solar energy is used for heating application and converts it into thermal energy. Solar air heater is the cheapest way of converting solar energy into thermal energy. Thermal performance of solar air heaters is comparably poor from solar water heaters. Thermal performance may be increased by increasing convective heat transfer coefficient. There are two way for increasing heat transfer coefficient either increase the area of absorbing surface by using fins or create the turbulence on the heat transferring surfaces The greatest advantage of solar energy as compared with other forms of energy is that it is clean and can be supplied without any environmental pollution.Over the past century fossil fuels have provided most of our energy because these are much cheaper and more convenient than energy from alternative energy sources and until recently environment pollution has been of little concern.

The major drawback with this resource is its low intensity, intermittent nature and non-availability during night. In spite of these limitations, solar energy appears to be the most promising of all the renewable energy resources. Solar energy is contemplated to have a wide range of applications including water heating, air heating, air-conditioning of buildings, solar refrigeration, photo-voltaic cells, green houses, photo-chemical, power generation, solar furnaces and photo-biological conversions to list a few. Out of these, the utilization of solar energy for power generation and heating/cooling of buildings is the subject of active research these days.

II. CONCEPT OF ARTIFICIAL ROUGHNESS

Thermo hydraulic performance of a solar air heater can be improved by providing artificial roughness on the absorber plate. The artificial roughness has been used extensively for the enhancement of forced convective heat transfer, which further requires flow at the heat-transferring surface to be turbulent. However, energy for creating such turbulence has to come from the fan or blower and the excessive power is required to flow air through the duct. Therefore, it is desirable that the turbulence must be created only in the region very close to the heat transferring surface, so that the power requirement may be lessened. This can be done by keeping the height of the roughness elements to be small in comparison with the duct dimensions. The key dimensionless geometrical parameters that are used to characterize roughness are:

1. Relative roughness pitch (p/e): Relative roughness pitch (p/e) is defined as the ratio of distance between two consecutive ribs and height of the rib
2. Relative roughness height (e/d): Relative roughness height (e/d) is the ratio of rib height to equivalent diameter of the air passage.
3. Angle of attack: Angle of attack is inclination of rib with direction of air flow in duct.
4. Shape of roughness element: The roughness elements can be two-dimensional ribs or three dimensional discrete elements, transverse or inclined ribs or V-shaped continuous or broken ribs with or without gap. The roughness elements can also be arc shaped wire or dimple or cavity or compound rib grooved. The common shape of ribs is square but different shapes like circular, semi-circular and chamfered have also been considered to investigate thermo hydraulic performance.
5. Aspect ratio: It is ratio of duct width to duct height. This factor also plays a very crucial role in investigating thermo hydraulic performance

III.EXPERIMENTAL DETAILS

Fig.1.1 Schematic diagram of Experimental Setup.

The schematic diagram of the test setup is shown in fig 1.1.The setup consists of a duct having artificially roughened absorber plate, heater, pipe line, centrifugal blower and instrumentations for measuring mass flow rate of air, pressure drop, temperature and voltage for heating the absorber plate. The various components of experimental setup are discussed below.

3.1 Air duct.

The most important part of the setup is the duct which was fabricated from plywood panels. The duct is 2600 mm long, 150 mm wide and 30 mm deep. The test section is 1200 mm long and has a cross section of 150 mm width ×30 mm depth. The entry and exit lengths were 800 mm and 600 mm, respectively. It may be noted that ASHRAE Standard [93–77] recommends minimum entry and exit length of $5\sqrt{WH}$ and $2.5\sqrt{WH}$, respectively. The sidewalls of duct were also made of thick plywood panels having smooth surface

3.2 Absorber plate

A 2mm thick aluminium sheet of 1200mm× 150mm size is used as an absorber plate. The lower surface of the plate is provided with artificial roughness with varying relative pitch (p/e).

3.3 Heater

A uniform heat flux up to a maximum of 1500W/m2 to the absorber plate is provided by a solar simulator. The power supply to the heater is controlled through an AC variac. To ensure all the heat flux is transferred to the duct and also to minimize the heat loss the duct is insulated on the other three sides except absorber plate side

3.4 Manometer.

An orifice meter connected with U- tube manometer is used to measure the air flow rate in the duct. A micro-manometer is used to measure the pressure drop across the test section.

3.5 Thermocouples

To measure the temperature of air and absorber plate at various locations calibrated chromel-alumel thermocouples are used.

IV.EXPERIMENTAL PROCEDURE

The test runs, to collect relevant heat transfer and flow friction data conducted under steady-state conditions. For

different airflow rates, the system was allowed to attain a steady state before the data were recorded. All the components of the setup and instrument are examined carefully for their proper operation. Artificially roughened absorber plate is installed and the test section is assembled. Heater is used for supplying energy for heating for one hour to the test section. After one hour the blower is switched on. No leakage in the joints of the duct and pressure tapping's is ensured. Control valve is used to adjust the mass flow rate. All the readings are taken once the mass flow rate is fixed. Tests for eleven values of mass flow rate of air is conducted in order to cover the entire range of Reynolds number. The following parameters are measured during experimentation:

a. Temperature of the absorber plate and air at inlet and outlet of the test section.
b. Pressure drop across the test section.
c. Pressure difference across the orifice meter.
d. Voltage and current supply to the heater.

Table 1.1.Range of parameters

Sr No	Parameters	Range
1.	Reynolds number(Re)	3000-8000
2.	Duct aspect ratio (W/B)	5
3.	Test-section length, L (mm)	1200
4.	Roughness height, wire diameter, e (mm)	1.7
5.	Hydraulic diameter of duct, D (mm)	50
6.	Relative roughness height, e/D	0.034
7.	Relative roughness pitch, p/e	10 to 40

The test runs to collect the relevant heat transfer data were conducted under steady state conditions. Eleven values of flow rate were used for each set of test. After each change of flow rate, the system was allowed to reach steady state before the data were recorded.

The experimental data includes thermocouple readings and air mass flow rates. This data have been reduced to obtain the average plate temperature, average air temperature, mass flow rate (m), velocity of air (V), heat supplied to the air (q), and heat transfer coefficient (h). The thermo physical properties of the air have been taken at the average plate fluid temperature.

4.1 Mean air and plate temperatures[15]

$T_f = \frac{(T1 + T2 + \cdots + T5)}{5}$	Where, T1-T5 is the temperature of air at various locations of air duct.
$T_p = \frac{T6 + T7 \ldots T10}{5}$	Where, T6-T10 is the temperature of plate at various location of absorber plate.

4.2 Mass flow rate[15]

The mass flow rate is calculated as follows,

$m = \rho c_d a_o \sqrt{\frac{2gH}{1-(a_o/a_1)^2}}$	Where, ρ, Density of air, kg/m3 c_d , Coefficient of discharge, 0.62 a_o, area of orifice, m2 a_1, area of pipe, m2 $H = h_m(\rho_w \vert \rho)$ h_m , is manometer reading

4.3 Velocity of air[15]

The velocity of air in the duct is calculated as follows,

$V = \frac{m}{\rho WB}$	Where, ρ, Density of air, kg/m3 W, width of duct, m B, height of duct, m

4.4 Heat transfer rate[15]

Useful heat gain to the air flowing in the duct is calculated as follows,

$q = mc_p(t_o - t_i)$	Where, m, mass flow rate, kg/s c_p, Specific heat of air, J/Kg k t_o , temperature of air at outlet,°C t_i , temperature of air at inlet, °C

4.5 Convective heat transfer co efficient[15]

Convective heat transfer coefficient for the test section is calculated as follows,

$h = \frac{q}{A_c(t_p - t_f)}$	A_c, area of absorber plate, m2 q, heat transfer rate t_p, average temperature of

	absorber plate, t_f, average temperature of fluid, °C

4.6 Nusselt number[15]
The Nusselt number is calculated from the following expression,

$Nu_r = \frac{hD_h}{k}$	Where, h, Convective heat transfer coefficient, (W/m2k) k, thermal conductive of air, W/m K Dh= Hydraulic diameter $= \frac{4WH}{2(W+H)}$

4.7 Reynolds number[15]
The Reynolds number is calculate as follows,

$R_e = \frac{VD_h}{\nu}$	Where, V, velocity of air, m/s ν= kinematic viscosity,m2/s

4.8 Friction factor[15]
The friction factor was determined from the following equations,

$f_r = \frac{D_h \Delta p}{2LV^2\rho}$	Where, Δp, Pressure drop L= test length, 1200mm ρ, Density of air, kg/m3

V.RESULT & DISCUSSION

5.1. Plate with transverse wires as artificial roughness.

The heat transfer characteristics of solar air duct roughened with transverse wires, computed on the basis of experimental data collected for various flow and roughness parameters, have been discussed below. The results have been compared with those obtained in case of smooth ducts operating under similar operating conditions to discuss the enhancement in Nusselt number

.Fig 1.2 shows the Nusselt number as a function of Reynolds number for relative roughness pitch (p/e) values of 10, 20, 30, 40 and for a fixed value of relative roughness height (e/D_h) of 0.034. It can be seen from the figures that for given value of roughness parameters, the Nusselt number monotonously increases with increase of Reynold number.. Due to separation of the flow at the transverse wires, reattachment of free shear layer occurs for (p/e) of 10 and maximum heat transfer coefficient occurs in the vicinity of the reattachment region. For relative roughness pitch (p/e) of 20, 30, 40 reattachment may not occur hence the values of heat transfer coefficient corresponds to these values of (p/e) are found to be minimum. At very low Reynolds number (less than 5000), it can be seen from fig.1.2 that the values of Nusselt number for smooth duct is nearly equal to that of roughened duct may be attributed to the fact that laminar sub layer thickness increases as the flow is retarded by roughness elements in Reynolds number region.
The results presented in re-plotted in fig. 1.2 to bring out the effect of relative roughness pitch on Nusselt number. It has been observed that with the increase in the value of (P/e), Nusselt number decreases. This is explained on the basis of flow separation. For higher (P/e) the flow which separates after each roughness element does not reattach before it reaches the succeeding roughness. Also, maximum heat transfer has been found to occur in the vicinity of a reattachment point. The maximum heat transfer occurred at (P/e) 10 because of higher Nusselt number at higher Reynolds number. Hence, heat-transfer coefficient will maximum at the same value

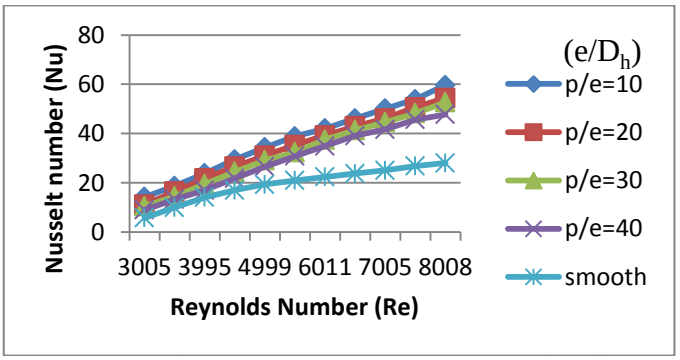

Fig.1.2. Variation of Nusselt number with Reynolds number for different values of (p/e) and for a fixed value of (e/D_h) for Transverse geometry

Fig 1.3 shows the variation of friction factor with Reynolds number for various relative roughness pitch (p/e) values of 10, 20, 30, 40 and for a fixed value of relative roughness height (e/D) of 0.034 from the graph it can be seen that the friction factor decreases with an increase of Reynolds number in all the cases due to the suppression of viscous sub-layer with increase in Reynolds number. Smooth plate has also been plotted in this figure for the purpose of comparison. It is observed that for a relative roughness pitch of 10 has maximum friction factor and that of 40 has minimum value.

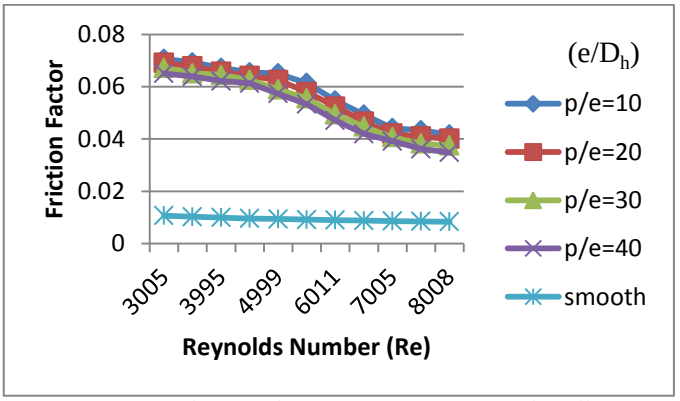

Fig.1.3. Variation of Friction factor with Reynolds number for different values of (P/e) and for a fixed values of (e/Dh) for Transverse geometry.

The Efficiency index of roughness plate with varying Reynolds number is shown in the below graph. From the graph it can be seen that the efficiency increases with the

increase of Reynolds number up to certain extent but after that it starts to stabilize

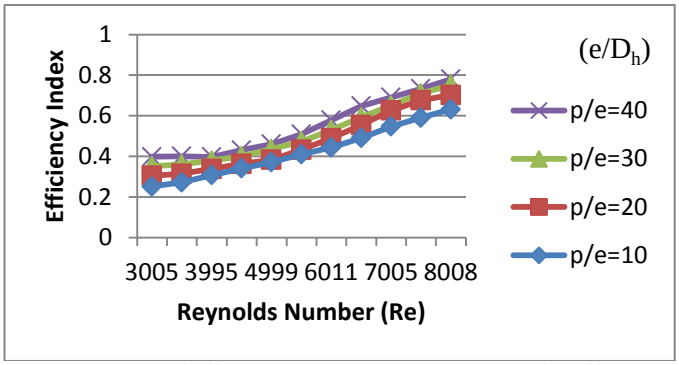

Fig.1.4. Variation of Efficiency Index with Reynolds number for different values of (P/e) and for a fixed values of (e/D_h) for Transverse geometry.

5.2 Plate with Single arc as artificial roughness

Fig 1.5. Form the figure the Nusselt number is found to be maximum for relative roughness pitch (P/e) value of 10. This can be explained on the basis of flow separation concept. Due to flow separation at the arc shaped geometry, reattachment of free shear layer occurs for (p/e) 10 and maximum heat transfer coefficients occurs in the vicinity of the reattachment region. The heat transfer coefficients corresponding to the values of relative roughness pitch (p/e) of 20, 30, 40 are found to be minimum due to no reattachment of free shear layer. The Nusselt number for that of the smooth plate is also given for the comparison purpose, from the figure it can be seen at low Reynolds number (less than 5000) the values of Nusselt number for smooth plate is nearly equal to that of roughened duct due to the fact that laminar sub layer thickness increases as the flow is retarded by roughness elements in Reynolds number region.

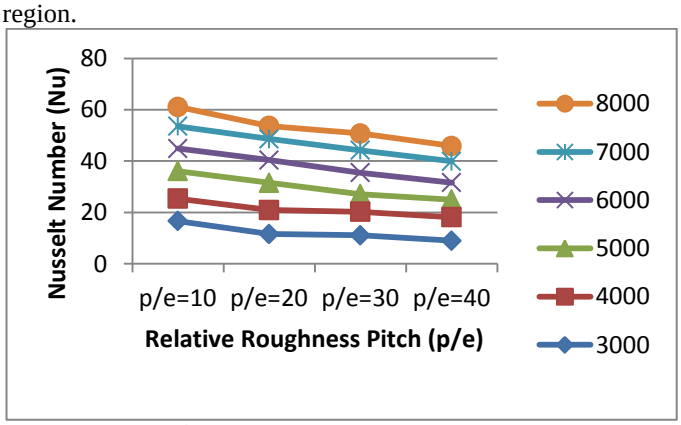

Fig.1.5. Variation of Nusselt number with Relative Roughness pitch (P/e) for different values of Reynolds number for Single arc geometry

Fig 1.6. shows the variation of Friction factor with Reynolds number for various relative roughness pitch (p/e) values of 10, 20, 30, 40 and for a fixed value of relative roughness height (e/D_h) of 0.034 for sing arc geometry. It can be seen from the graph that the friction factor decreases with an increase of Reynolds number in all the cases. For the purpose of comparison friction factor of smooth plate is also presented in the plot. It can be observed that for a relative roughness pitch of 10 has maximum friction factor and that of 40 has minimum value

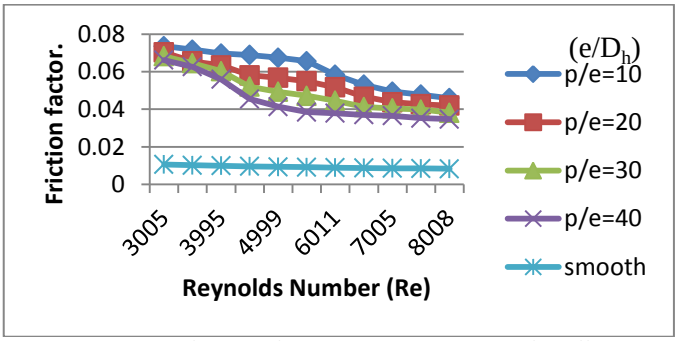

Fig.1.6. Variation of Friction factor with Reynolds number for different values of (P/e) and for a fixed values of (e/D_h) for Single arc geometry

Fig.1.7. shows the variation Friction factor with Relative Roughness pitch (P/e) for different values of Reynolds number for Single arc geometry. It has been observed that with the increase in the (p/e) values, friction factor of single arc geometry decreases. The maximum friction accurse at relative roughness pitch of (p/e) of 10 for lower Reynolds number.

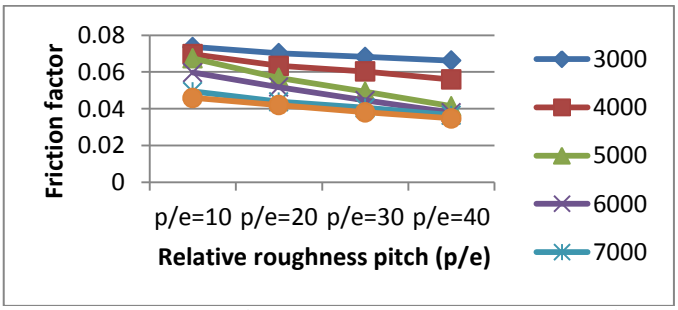

Fig.1.7. Variation Friction factor with Relative Roughness pitch (P/e) for different values of Reynolds number for Single arc geometry

Fig.1.8. shows the variation of Efficiency Index with Reynolds number for different values of (P/e) and for a fixed values of (e/D_h) for Single arc geometry. From the graph it can be seen that the efficiency increases as the Reynolds number increases for all the relative roughness pitch (P/e) values. The maximum efficiency is found to be at (p/e) values of 40 and minimum for (p/e) value of 10

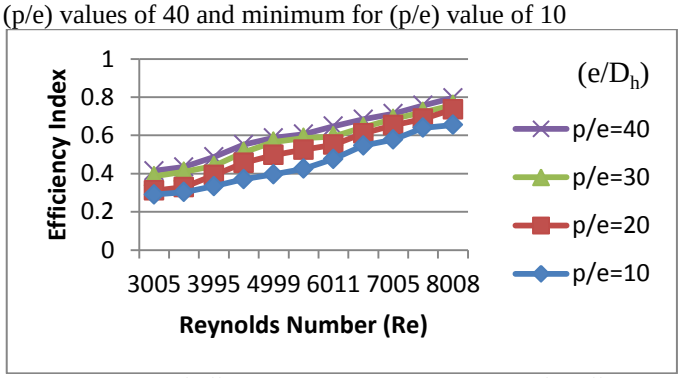

Fig.1.8. Variation of Efficiency Index with Reynolds number for different values of (P/e) and for a fixed values of (e/D_h) for Single arc geometry.

5.3 Plate with Double Arc as artificial roughness

Fig.1.9 shows Variation of Friction factor with Reynolds number for different values of (P/e) and for a fixed values of (e/D_h) for Double arc geometry. The friction factor decreases with increase in Reynolds number for all the values of (p/e), this is explained on the basis of flow separation as explained above in the earlier cases. The maximum friction factor is observed for relative roughness pitch of 10 and minimum for 40.Figure.4.16. shows the

variation of Friction factor with Relative Roughness pitch (P/e) for different values of Reynolds number for Double arc geometry. It is observed that with the increase in the value of (p/e) the friction factor decrease. The maximum pressure drop occurs at (p/e) 10 because of higher friction factor at lower Reynolds number

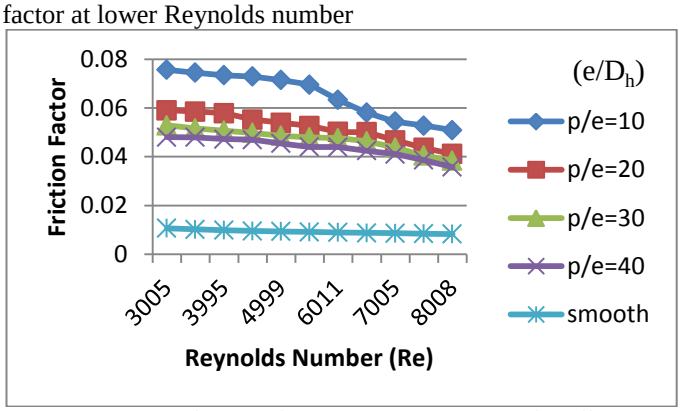

Fig.1.9. Variation of Friction factor with Reynolds number for different values of (P/e) and for a fixed values of (e/D_h) for Double arc geometry

Fig 1.10 shows the variation of effect of friction factor on the relative roughness pitch it decreases as the friction factor increases.

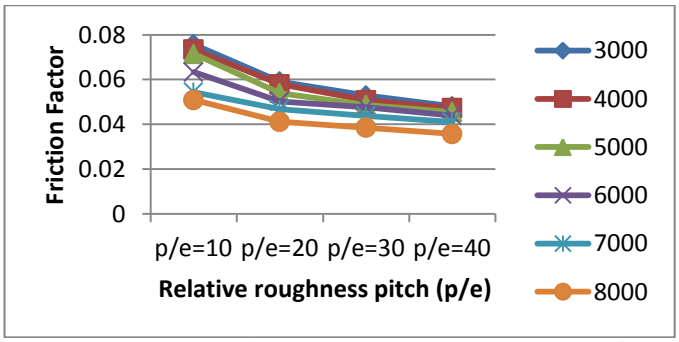

Fig.1.10. Variation Friction factor with Relative Roughness pitch (P/e) for different values of Reynolds number for Double arc geometry

The efficiency Index of roughness plate with double arc geometry is plotted in the fig1.11. It is seen that the efficiency increases with the increase in Reynolds number. The variation of Efficiency index with Relative Roughness pitch (P/e) for different values of Reynolds number for Double arc geometry. It is observed that with increase in the value of p/e, efficiency of Double arc geometry increases. The maximum efficiency occurred at (p/e) 40 at higher Reynolds number.

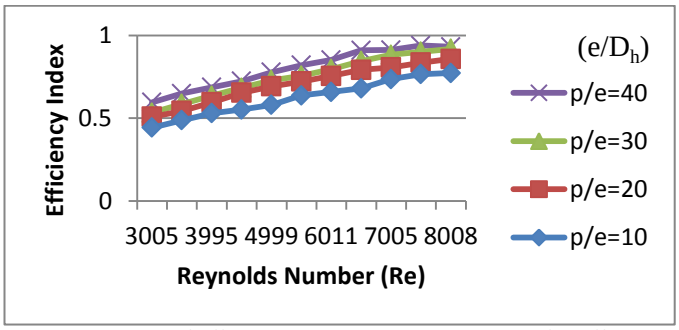

Fig.1.11. Variation of Efficiency Index with Reynolds number for different values of (P/e) and for a fixed values of (e/D_h) for Double arc geometry.

5.4 Comparison of Transverse, Single arc, Double arc roughness geometries.

Fig1.12 shows the variation in Nusselt number as a function of Reynolds number for different roughness geometries. Considerable jump in the Nusselt number can be seen in all the cases as compared to the Smooth surface. Plot reveals that the value of Nusselt number is highest in case of Double arc roughness and lowest in case of Transverse ribs for all the values of Reynolds number.

On the basis of this observation one can choose preferably double arc shape roughness to achieve higher heat transfer rates. Since Transverse ribs has only one secondary flow cell while single arc got two secondary flow cells and double arc roughness can generate multiple secondary flow cells and therefore double arc roughness shows maximum heat transfer augmentation.

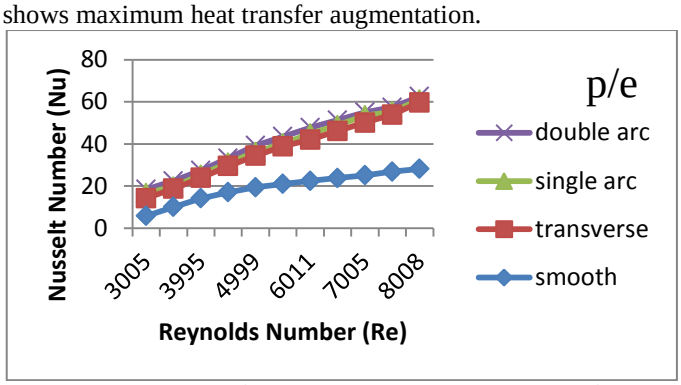

Fig.1.12. Comparison of Nusselt number with Reynolds number for different roughness geometries for fixed value of Relative roughness pitch (p/e=10)

Fig 1.13.shows the comparison of Nusselt number with Relative Roughness pitch (P/e) for different roughness geometries and for fixed value of Reynolds number. From the graph it can be seen that the Nusselt number is highest for relative roughness pitch (p/e) of 10 for all the roughness geometries considered in the present work. It is highest for (p/e) value of 10 for double arc roughness geometry and lowest for (p/e) value of 40 for transverse geometry.

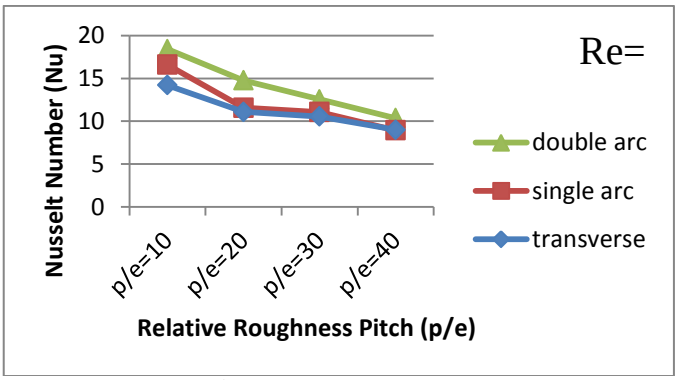

Fig.1.13. Comparison of Nusselt number with Relative Roughness pitch (P/e) for different roughness geometries for fixed value of Reynolds number

Fig.1.14. shows the comparison of Efficiency Index with Reynolds number for different roughness geometries for fixed value of Relative roughness pitch (p/e=10), from the graph it can be seen that the efficiency is highest for Double arc roughened plate and lowest for Transvers roughened plate. More secondary flows are generated in the Double arc roughened plate than in the Single arc roughened plate and lowest in case of Transvers plate hence the efficiency is highest for Double arc roughened plate.

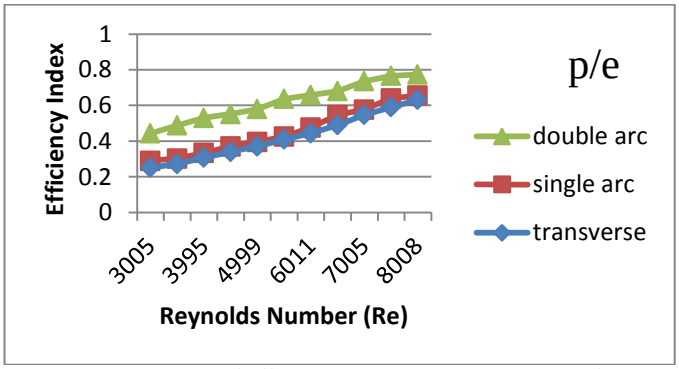

Fig.1.14. Comparison of Efficiency Index with Reynolds number for different roughness geometries for fixed value of Relative roughness pitch (p/e=10)

Fig.1.15. shows the comparison Efficiency Index with Relative Roughness pitch (P/e) for different roughness geometries for fixed value of Reynolds number. From the graph it can be seen that the efficiency index increases with the increase in relative roughness (p/e) values for all the roughness geometries considered in the present work. It is found to be highest for (p/e) value of 40 for Double arc roughened plate and lowest for (p/e) value of 10 for transverse roughened plate

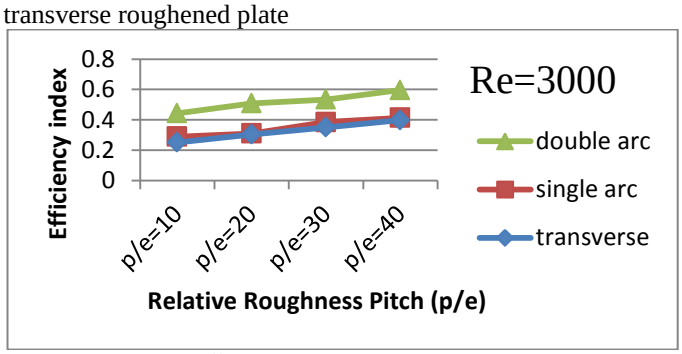

Fig.1.15. Comparison Efficiency Index with Relative Roughness pitch (P/e) for different roughness geometries for fixed value of Reynolds number

VI.CONCLUSION

1.Use of artificial roughened surface with different type of roughness geometries is found to be the most effective technique to enhance the heat transfer ratesfrom the heated surface to flowing fluid at the cost of moderate rise in fluid friction.

2.In the entire range of Reynolds Number it is found that Nusselt number increases and friction factor decreases with an increase of Reynolds number in all the cases, Nusselt number and friction factor are significantly higher as compared to those obtained for smooth absorber plates. This is due to the distinct change in the fluid flow characteristics as a result of roughness that causes flow separation, reattachment and the generation of secondary flows

3.For all the three roughness geometries (transverse, single arc, double arc) it was found that the Nusselt number increases as Reynold number increases, the maximum value of Nusselt number is found corresponding to relative roughness pitch (p/e) of 10, while the minimum value of Nusselt number corresponds to relative roughness pitch (p/e) of 40. The friction factor decrease as the Reynolds number is increased for all the relative roughness pitch (p/e) value, it is found to be maximum for relative roughness pitch (p/e) of 10 and minimum for (p/e) of 40

4.The efficiency index increases as the Reynolds number is increased for all the values of relative roughness pitch (p/e), it was found to be maximum for (p/e) value of 40 and minimum for (p/e) value of 10. Also the efficiency index was found to be increases with increase of (p/e) values and it was found to be maximum for (p/e) of 40 and for higher Reynolds number of 8000, and was found to be minimum for (P/e) value of 10 and for lower Reynolds number of 3000

5.The comparison of transvers, single arc, double arc, and smooth absorber plate shows that the Nusselt number, friction factor and efficiency index is highest for double arc shaped roughness followed by single arc, transvers and least for smooth absorber plate.

6.It has also been observed that a lower Reynolds number (less than 5000) a smooth plate and an artificially roughened plate have very less variation of heat transfer.

7.It can be concluded that the maximum heat transfer is found to be in double arc roughness absorber plate than other shapes.

ACKNOWLEDGMENT

I wish to express my sincere gratitude to **Dr. V. N. NITNAWARE**, Principal and **Prof. A.A. Bagade** H.O.D of Mechanical Engineering Department, of Dr. D.Y.Patil School Of Engineering Academy, Ambi for providing me an opportunity to present a paper on **"Enhancement of heat transfer rate and thermal efficiency of solar air heater by using flow turbulators on absorber plate."** This Paper is incomplete without the guidance of many peoples.

I sincerely thank to my project guides **Prof. S.K Bhor** and **Prof. Vikram Bharath B R** for guidance in carrying out this paper. I also wish to express my gratitude to **Prof. R.R. Katwate (ME Co-ordinator)** who has been constantly a source of encouragement for this paper work. I wish to avail myself of this opportunity, express a sense of gratitude and love to my friends and my beloved parents for their manual support, strength, and help for everything.

REFERENCES

[1] Abdul-Malik EbrahimMomin, J. S. Saini, S. C. Solanki, Heat transfer and friction insolar airheater duct with V-shaped rib roughness on absorber plate, International Journal of Heat and Mass Transfer 45 (2002) 3383-3396.

[2] J.C. Han, Heat transfer and friction characteristics in rectangular channels with rib turbulators, ASME J. Heat Transfer 110 (1988) 321-328.

[3] N. Sheriff and P. Gumley, Heat Transfer and Friction Properties of surface with Discrete Roughness, International Journal of Heat and Mass Transfer (9) (1996) 1297-1320.

[4] Santosh B. Bopche and Madhukar S. Tandale, Experimental Investigation oh heat and friction characteristics of a turbulatorroughned solar air heater duct, International Journal of Heat and Mass Transfer 52 (2009) 2834-2848.

[5] M. M. Sahu and J. L. Bhagoria, Augmentation of heat transfer coefficient by using 90° broken transverse ribs on absorber plate of solar air heater, Renewable Energy 30 (2005) 2057-2073.

[6] RajkumarAhirwar and A .R. Jaurker, Study of heat transfer characcteristics of V-shaped artificially roughened solar air heater, VSRD International journal of Mechanical, Automobile and Production

Engineering, Vol. 2 No. 10 December 2012, ISSN No. 2249-8304.

[7] ApurbaLayek J.S. Saini S.C. Solanki, Heat tramsfer and friction characteristics for artificially roughned ducts with compound turbulators, International Journal of Heat and Mass Transfer 50 (2007) 4845-4854.

[8] R.P. Saini and JitendraVerma, Heat transfer and friction factor correlations for a duct having dimple-shape artificial roughness for solar air heaters, Energy 33 (2008) 1277-1287.

[9] S.V. Karmare, A.N. Tikekar, Heat transfer and friction factor correlation for artificially roughned duct with metal grit ribs, International Journal of Heat and Mass Transfer 50 (2007) 4342-4351.

[10] A. R. Jaurker, J. S. Saini, B. K. Gandhi, Heat transfer and friction characteristics air heater duct using rib-grooved artificial roughness, Solar energy 80 (2006) 895-907.

[11] A. M. Lanjewar, J. L. Bhagoria and R. M. Sarviya, Enhancement of heat transfer ratio in a solar air duct with W-shaped roughned absorber plate, Journal of environmental Research And Development, Vol.5 No.1, July-September 2010.

[12] Varun, R. P. Saini, S. K. Singal, Investigation of thermal performance of solar air heater having roughness element as a combination of inclined and transverse ribs on the absorber plate, Renewable Energy 33 (2008) 1398-1405.

[13] Anil Kumar, R. P. Saini, J. S. Saini, Experimental Investigation on Thermohydraulic performance due to flow- attack- angle in Multi V ribs with gap in a rectangular duct of solar air heaters, Journal of sustainable Energy & environment 4 (2013) 1-7.

[14] Manish Kumar Chauhan, Varun, SachinChaudhary, Performance evaluation of roughned solar air heater having M-shaped as roughness geometry on the absorber plate, International Journal of Energy and environment, Volume 3, Issue 6, 2012 pp.881-894.

[15] Prashant Kumar Kori, A. R. Jaurker, Study of heat transfer characteristics of W-shaped ribbed solar air heater, VSRD International journal of Mechanical, Automobile and Production Engineering, Vol. 3 issue IX September 2013, e-ISSN : 2249-8304, p-ISSN: 2319-2208.

[16] ApurbaLayek, Optimal thermo-hydraulic performance of solar air heater having chamfered rib-groove roughness on absorber plate, , International Journal of Energy and environment, Volume 1, Issue 4, 2010 pp.683-696.

[17] P. Promvonge, C. Khanoknaiyakarn, S. Kwankaomeng, C. Thianpong, Thermal behavior in solar air heater channel fitted with combined rib and delta-winglet, International Communications in Heat and Mass transfer 38 (2011) 749-756.

[18] S. S. Pawar, Dr. D. A. Hindolia, Dr. J. L. Bhagoria, Enhancemetn of heat transfer coefficient using Diamond shaped roughness on the absorber plate of solar air heater, International Journal of engineering Research and Applications ISSN: 2248-9622, Vol 3,